Radiology

Shoulder US: Anatomy, Technique, and Scanning Pitfalls[1]

Jon A. Jacobson, MD

The accuracy of shoulder ultrasonography (US) is largely dependent on the US examination technique. It is essential that the individual performing the US examination has an understanding of pertinent anatomy, such as bone surface anatomy and tendon orientation. It is also important to be familiar with imaging pitfalls related to US technique, such as anisotropy. In this article, shoulder US scanning technique, as well as related anatomy and scanning pitfalls, will be reviewed. The use of a protocol-driven shoulder US examination is important to ensure a comprehensive and efficient evaluation. An on-line video tutorial demonstrating a shoulder US also accompanies this article.

Supplemental material: *http://radiology.rsna.org/lookup/suppl/doi:10.1148/radiol.11101082/-/DC1*

[1]From the Department of Radiology, University of Michigan Medical Center, 1500 E Medical Center Dr, TC-2910L, Ann Arbor, MI 48109. Received July 7, 2010; revision requested August 13; revision received January 21, 2011; final review by the author January 30. **Address correspondence to** the author (e-mail: *jjacobsn@umich.edu).*

The shoulder is commonly evaluated with ultrasonography (US), with which various rotator cuff diseases can be effectively diagnosed, including tendinosis, tendon tear, and bursitis (1,2). Accuracies in the diagnosis of rotator cuff tears can reach 100% for full-thickness tears (3) and 91% for partial-thickness tears (4); however, accuracy can be variable, depending on the skill and experience of the individual performing the US examination (5). When the shoulder is evaluated with US, a scanning protocol is followed that includes a checklist of key structures (Table). Such an evaluation is critical for a thorough, comprehensive, and efficient examination. It has also been shown that patients with shoulder disease do not indicate focal symptoms that directly correlate with the location of disease; therefore, a focused ultrasound alone is inadequate (6). The first step to developing a comprehensive shoulder US examination is a thorough understanding of the anatomy. In this review of shoulder US technique, key shoulder anatomy will be emphasized. This will be followed by a description of step-by-step US technique that can be effective in evaluating the shoulder. This is accompanied by a video showing a demonstration of shoulder US (Movie [online]). Last, several common and important pitfalls of a shoulder US technique will be emphasized.

Anatomy

The shoulder is a synovial articulation between the glenoid and the humeral head in which the shallow glenoid articulation is deepened an additional 50% by the fibrocartilaginous labrum that forms a rim around the perimeter of the glenoid (7). Both the glenoid and the humeral head are covered by a layer of hyaline articular cartilage. Four muscles attach as tendons onto the proximal humerus and make up the rotator cuff: supraspinatus, subscapularis, infraspinatus, and teres minor (Fig 1). The supraspinatus is located in the suprascapular fossa of the scapula and inserts onto the greater tuberosity of the proximal humerus. The subscapularis is located anterior to the scapula and inserts onto the lesser tuberosity of the proximal humerus. The infraspinatus is located posterior to the scapula inferior to the scapular spine and inserts onto the posterior aspect of the greater tuberosity, and the teres minor is located just inferior to the infraspinatus and also inserts onto the greater tuberosity.

By taking a closer look at the greater tuberosity, familiarity with facet anatomy and bone landmarks can assist in correctly identifying the individual tendons of the rotator cuff (Fig 2). The greater tuberosity consists of three facets moving from anterior to posterior: a superior facet, a middle facet, and an inferior facet. The supraspinatus is approximately 23 mm in width (measured anterior to posterior), of which the anterior 13 mm inserts onto the superior facet and the posterior 10 mm inserts onto the anterior aspect of the middle facet (8). The infraspinatus is approximately 22 mm in width (measured anterior to posterior) and inserts onto the middle facet of the greater tuberosity, superficially overlapping the supraspinatus tendon by 10 mm (8). It should be noted that some variability in the distal cuff insertion may exist, as anterior extension of the infraspinatus tendon over the superior facet and anterior extension of the supraspinatus tendon to the lesser tuberosity have been described (9). The teres minor attaches onto the inferior facet of the greater tuberosity, located posterior. Tendon attachment to the greater tuberosity is by means of a fibrocartilaginous enthesis (10).

One should also be familiar with the anatomy of the supraspinatus footprint at the greater tuberosity, as many rotator cuff tears involve this area (Fig 3). If one follows the articular cartilage over the humeral head from medial to lateral, the cartilage will terminate at a sulcus formed between the humeral head and greater tuberosity. Just lateral to the hyaline articular cartilage termination is a 1.5–1.9-mm bare area devoid of cartilage, and immediately lateral one will see the articular fibers of the rotator cuff attach to the greater tuberosity (11). Beyond this sulcus, the distal supraspinatus attachment occurs over a distance of approximately 12 mm from medial to lateral on the greater tuberosity facet, termed the *supraspinatus footprint* (11). A similar anatomic appearance is seen at the infraspinatus attachment; however, the sulcus or bare area between the termination of the hyaline articular cartilage and the middle facet of the greater tuberosity is wider (13.9 mm) and is a site of cortical irregularity with cysts that may be considered a normal variation (12,13). The subscapularis attaches to the lesser tuberosity, with superficial fibers extending over the bicipital groove as the transverse humeral ligament.

The rotator interval is a space between the anterior leading edge of the supraspinatus tendon and the superior edge of the subscapularis tendon. In this space, the long head of the biceps brachii tendon becomes intraarticular as it courses toward the supraglenoid tubercle of the scapula. The rotator interval also allows a direct communication between the glenohumeral joint and the subscapularis recess. In the rotator interval, the coracohumeral ligament is seen superficial to the biceps brachii tendon, and the superior glenohumeral ligament is seen medial, forming a slinglike band that surrounds the biceps brachii tendon (14).

Essentials

- A protocol-driven to approach to shoulder US technique will ensure a comprehensive and efficient examination.
- Understanding bone surface anatomy is important to identify tendon orientation.
- Imaging should be aligned in short and long axis of a tendon.
- Anisotropy must be recognized and avoided.

Published online
10.1148/radiol.11101082 **Content codes:** MK US

Radiology 2011; 260:6–16

Potential conflicts of interest are listed at the end of this article.

There are several other anatomic structures about the shoulder that deserve mention. First is the acromioclavicular joint, which is also a synovial articulation. A fibrocartilage disc is located in the acromioclavicular joint, which degenerates and usually disintegrates by the age of 40 years (15). Another anatomic structure is the subacromial-subdeltoid bursa. This extraarticular synovial space is primarily located between the supraspinatus tendon and the coracoacromial arch, but can extend anterior over the bicep brachii long head and subscapularis tendons and posterior over the infraspinatus tendon. The coracoacromial arch is located over the supraspinatus tendon and subacromial-subdeltoid bursa and consists of the coracoid, the coracoacromial ligament, and the acromion.

Shoulder US Protocol

Step No.	Protocol
1	Biceps brachii tendon, long head
2	Subscapularis and biceps brachii tendon, subluxation/dislocation
3	Supraspinatus and rotator interval
4	Acromioclavicular joint, subacromial-subdeltoid bursa, and dynamic evaluation for subacromial impingement
5	Infraspinatus, teres minor, and posterior labrum

Figure 1

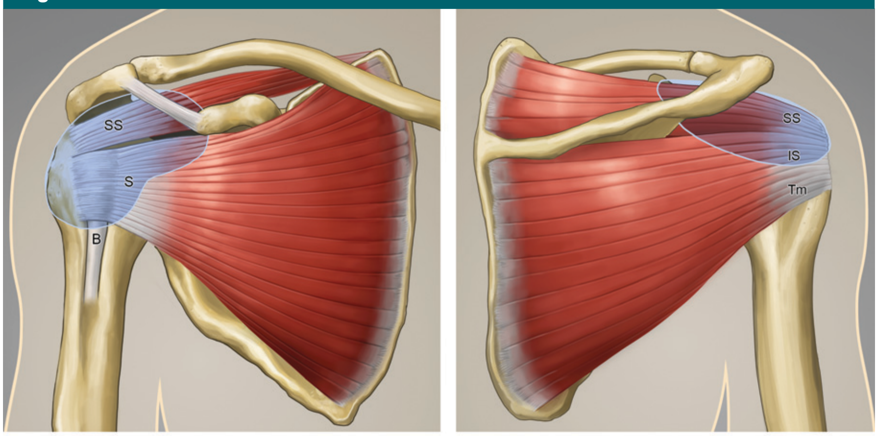

a. **b.**

Figure 1: Shoulder anatomy. Illustrations of **(a)** anterior and **(b)** posterior shoulder show supraspinatus *(SS)*, infraspinatus *(IS)*, subscapularis *(S)*, teres minor *(Tm)*, and long head of the biceps brachii tendon *(B)*. Subacromial-subdeltoid bursa is overlying the rotator cuff (light blue). (Image courtesy of Carolyn Nowak, Ann Arbor, Mich.)

Technique

General Comments

For US evaluation of the shoulder, the author prefers to scan facing the front of the patient rather than behind the patient. The patient is sitting on a stool (without wheels) equipped with a short back support, which allows patient stability and US access to all aspects of the shoulder. The author also prefers to sit on a stool with wheels to allow mobility. The sonographer should perform the examination in a comfortable position so as to avoid developing work-related injuries (16). To reduce strain, the sonographer should ideally be positioned so that his or her shoulder is higher than the patient's shoulder, and the elbow should be close to the body rather than extending the arm toward the patient. The transducer should also be held at its end, stabilizing the transducer by resting either the edge of the hand or the little finger on the patient, which also reduces strain on the shoulder and allows fine motor control during US scanning.

At the beginning of the examination, obtaining a brief history can provide clues to the underlying disease. For example, it is common for patients with rotator cuff disease to describe pain that radiates to the elbow and often awakens them at night. Information with regard to trauma, mass, or infection is also helpful. A patient older than age 40 years of age is more likely to have a rotator cuff tear compared with a younger patient, who is more likely to have labral disease. At the end of the US examination, the author prefers to inform the patients of their results and answer questions. This interaction can make the US examination a positive experience for the patient.

From beginning to end, most shoulder US examinations can be completed in less than 10 minutes. If the shoulder is normal, the time required is often less than 5 minutes, although this depends on the experience of the sonographer. It is critical that a protocol be followed to provide a comprehensive evaluation, as a focused examination of the shoulder is considered inadequate. At the end of the protocol, it is always important to ask the patient if he or she has focal symptoms; focused scanning at that site may reveal disease not evaluated during the routine shoulder protocol.

With regard to US equipment, image resolution improves as the frequency of the transducer increases, but this is at the expense of depth penetration. In general, an ultrasound probe of at least 10 MHz will suffice. For an average-sized patient, a transducer of 12–15 MHz produces detailed images with high resolution, while uncommonly a 9-MHz transducer is required for extremely large patients to allow depth penetration, but this is at the expense of lower resolution. The transducer should be linear (with a flat rather than curved surface) so that the sound beam propagates through the soft tissues in a similar

Figure 2

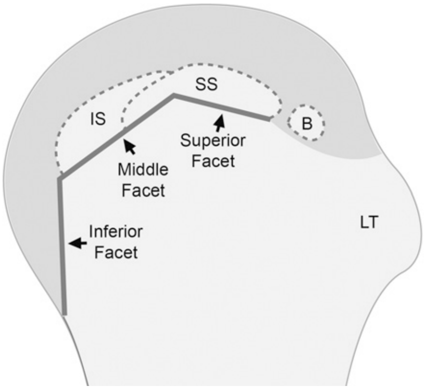

Figure 2: Greater tuberosity facets. Illustration of lateral aspect of proximal humerus shows location of supraspinatus *(SS)* and infraspinatus *(IS)* tendon attachments relative to the greater tuberosity facets. *B* = long head of biceps brachii tendon, *LT* = lesser tuberosity. Right side of image is anterior. (Image courtesy of Carolyn Nowak, Ann Arbor, Mich.)

Figure 3

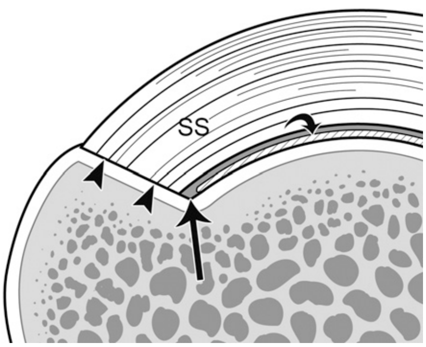

Figure 3: Supraspinatus footprint. Illustration of long-axis section through supraspinatus tendon *(SS)* shows footprint attachment at greater tuberosity (arrowheads). Hyaline articular cartilage covers the humeral head (curved arrow). Note sulcus between hyaline cartilage and tendon attachment (straight arrow).

linear fashion. This will ensure that the sound beam is directed perpendicular to the tendon fibers and minimize anisotropy, which causes the tendon to appear artifactually hypoechoic. The true US characteristics of a normal tendon are only seen when the tendon is imaged perpendicular to the sound beam. If the bone cortex under a tendon is clearly defined and hyperechoic, that

Figure 4

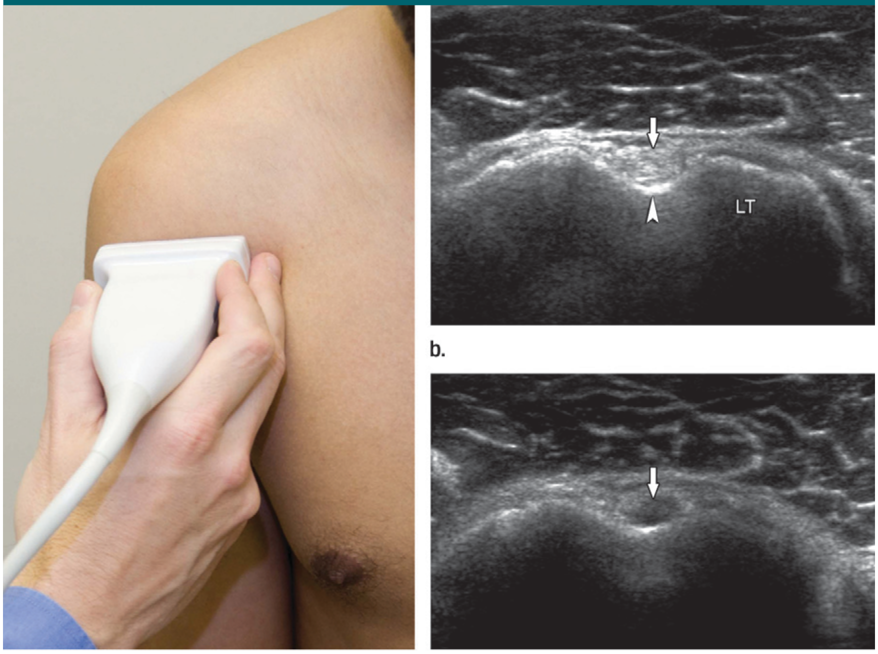

a. b. c.

Figure 4: Long head of the biceps brachii tendon (short axis). **(a)** Transducer placement. **(b)** Corresponding US image shows long head of the biceps brachii tendon (arrow) in the bicipital groove (arrowhead). *LT* = lesser tuberosity. Right side of image is medial. **(c)** US image shows hypoechoic appearance of the tendon (arrow) due to anisotropy when not imaged perpendicular to the sound beam.

Figure 5

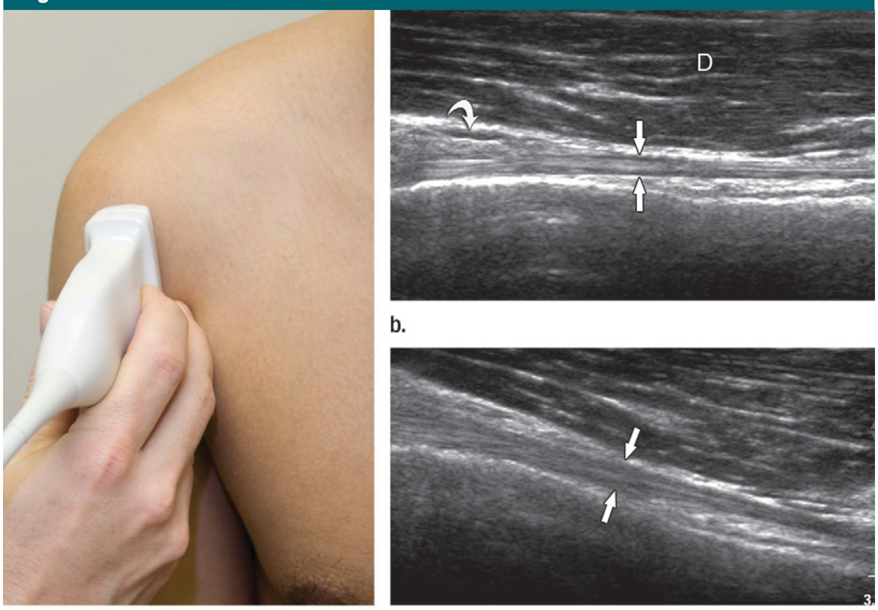

a. b. c.

Figure 5: Long head of the biceps brachii tendon (long axis). **(a)** Transducer placement. **(b)** Corresponding US image shows long head of the biceps brachii tendon (straight arrows) in long axis. *D* = deltoid muscle. Curved arrow = subacromial-subdeltoid bursa. Right side of image is distal. **(c)** US image shows hypoechoic appearance of the tendon (arrows) due to anisotropy when not imaged perpendicular to the sound beam.

Figure 6

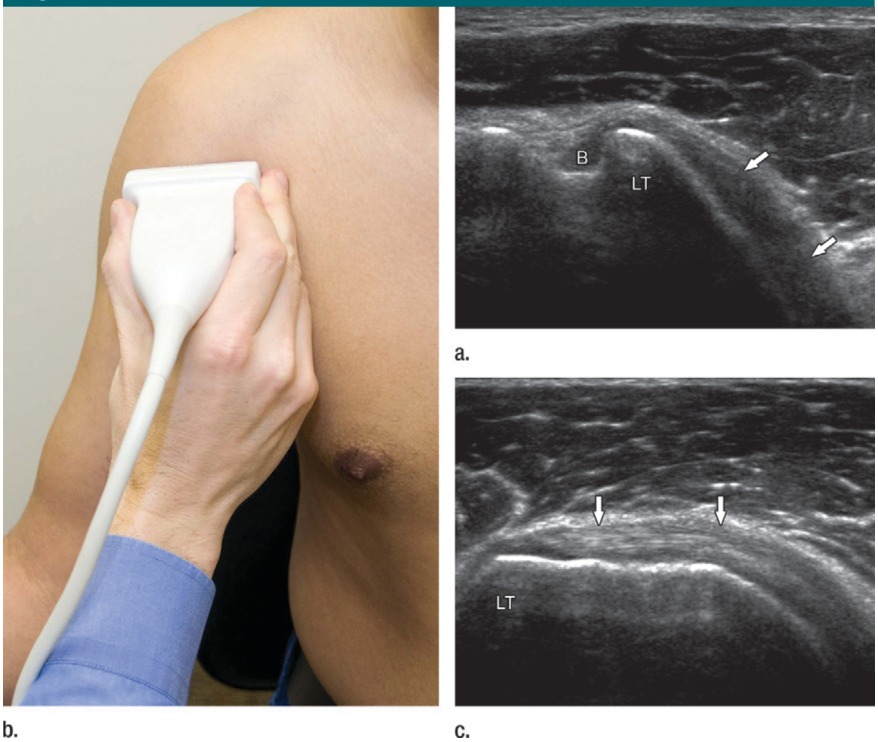

Figure 6: Subscapularis tendon (long axis). **(a)** Centered over lesser tuberosity *(LT)*, US image shows subscapularis tendon (arrows) artifactually hypoechoic from anisotropy. *B* = biceps brachii tendon. Right side of image is medial. **(b)** Transducer placement with shoulder externally rotated. **(c)** Corresponding US image shows hyperechoic and fibrillar subscapularis tendon (arrows). *LT* = lesser tuberosity.

indicates the sound beam is perpendicular to the cortex and also therefore perpendicular to the overlying tendon, minimizing anisotropy.

The following demonstrates the sequential steps that the author follows to evaluate the shoulder with US: The basic objectives for each step are to *(a)* identify the tendon of interest, *(b)* image the tendon in two planes (long and short axis), *(c)* eliminate artifact by directing the ultrasound beam perpendicular to the tendon, and *(d)* diagnose disease. These same objectives also apply to other imaging, such as magnetic resonance (MR) imaging. Indeed, oblique imaging of a tendon (rather than in short and long axis) is a telltale sign of poor technique, which is readily apparent even on static US images. With regard to documentation of imaging, each structure on the checklist should be imaged in two planes. If disease is identified, more images are obtained to further characterize and document any abnormality. If available, cine clips of each structure provide information that can be later reviewed at a workstation.

Step 1: Biceps brachii tendon, long head.—The patient is asked to place his or her hand palm up on the lap. The transducer is placed in the axial plane on the body over the anterior shoulder (Fig 4a). The bicipital groove is identified by its characteristic bone contours, with the bone surface appearing hyperechoic with posterior acoustic shadowing. Within the bicipital groove lies the long head of the biceps brachii tendon, seen in short axis (Fig 4b). Because the biceps tendon is coursing deep away from the skin surface, it is common for the tendon to appear artifactually hypoechoic from anisotropy (Fig 4c). This artifact is eliminated by rocking (or toggling) the transducer along the long axis of the tendon so that the sound beam is angled superiorly. The normal tendon will then appear hyperechoic and fibrillar. The long head of the biceps brachii tendon is followed proximally to where the bicipital groove becomes shallow and then distal to the level of the pectoralis major tendon, which is identified coursing over the biceps tendon to insert on the lateral aspect of the bicipital groove. The transducer is then turned 90° to visualize the biceps tendon in long axis (Fig 5a). Transducer pressure distally is usually needed to aim the ultrasound beam cephalad and perpendicular to the biceps tendon, which will appear hyperechoic and fibrillar (Fig 5b). If the biceps brachii tendon is oblique to the sound beam, it will appear hypoechoic from anisotropy (Fig 5c). Some US machines have beam-steering capabilities that can also be used to reduce anisotropy. The biceps tendon is evaluated for abnormalities such as tendinosis and tendon tear, as well as surrounding joint fluid or tenosynovitis. Only a sliver of fluid posterior to the biceps tendon is considered physiologic.

Step 2: Subscapularis and biceps tendon subluxation/dislocation.—With the patient's hand remaining palm up on his or her lap, the transducer is again placed over the anterior shoulder in the axial plane to visualize the bicipital groove (Fig 4a). The transducer is then centered over the lesser tuberosity at the medial aspect of the bicipital groove. The subscapularis tendon will be seen in long axis coursing anterior toward the lesser tuberosity and will appear artifactually hypoechoic from anisotropy (Fig 6a). The patient is then asked to externally rotate the shoulder (Fig 6b). As the lesser tuberosity rotates laterally, the subscapularis located inferior to the coracoid is pulled lateral, eliminating anisotropy as its fibers are oriented perpendicular to the sound beam in long axis (Fig 6c). The transducer is moved superior and inferior to ensure complete evaluation. Care must be taken to adequately visualize the most superior aspect of the subscapularis, as most subscapularis tears associated with supraspinatus tears will involve this area. The transducer is then rotated

90° (Fig 7a) to visualize the subscapularis tendon in short axis (Fig 7b). The hypoechoic subscapularis muscle, which interdigitates with its multiple hyperechoic tendons, or tendon anisotropy should not be misinterpreted as disease (Fig 7c). The US transducer is again rotated 90° along the long axis of the subscapularis and moved laterally over the bicipital groove to ensure that the long head of the biceps brachii tendon is normally located in the bicipital groove. Partial displacement of the biceps tendon from the bicipital groove is termed *subluxation*, while complete medial displacement is termed *dislocation*. Such abnormal position of the biceps tendon may only occur transiently during external shoulder rotation.

Step 3: Supraspinatus and rotator interval.—The goal in imaging the supraspinatus tendon, similar to other structures, is to visualize the tendon exactly in long and short axis. It should be noted that rotation of the proximal humerus will change the tendon orientation and therefore the imaging plane of the supraspinatus. This same issue also occurs when imaging the supraspinatus tendon with MR imaging. The key to understanding the correct imaging plane of the supraspinatus is to recognize the location of the greater tuberosity and to identify the bone landmarks. The location of the greater tuberosity will change depending how the shoulder is positioned.

Initial descriptions of shoulder US technique used the Crass position for evaluation of the supraspinatus, where the dorsal aspect of the ipsilateral hand is placed behind the back (17). This hyperextended and internally rotated position pulls the supraspinatus tendon out from under the acromion. In this position, the greater tuberosity is located directly anterior; to obtain a long-axis view of the supraspinatus, the transducer is simply placed in the sagittal plane over the anterior shoulder. The primary advantage of the Crass position is easy and reliable localization of the greater tuberosity; however, disadvantages include poor visualization of the rotator interval and patient discomfort. Because of this, the author uses a modified Crass position, where the patient's ipsilateral hand is placed on the closest hip or buttock region (Fig 8a), which allows easy visualization of the rotator interval with little patient discomfort (18). In this position, the greater tuberosity is now located more lateral than with the Crass position as the degree of internal rotation is decreased. The long-axis plane of the supraspinatus is approximately 45° in a plane inferior and lateral from the acromioclavicular joint. The patient's elbow should point posterior while in the modified Crass position so that the rotator interval can be adequately visualized.

Once the patient is in the modified Crass position, the supraspinatus tendon is visualized in long axis (Fig 8b). This long-axis view of the supraspinatus is an important view in that the anatomic surfaces of the supraspinatus tendon (intraarticular, bursal, greater tuberosity) are identified, allowing accurate characterization of a tear (articular, bursal, intrasubstance, or full-thickness). Two crucial points must be made with regard to supraspinatus tendon evaluation. The first is that the entire width of the greater tuberosity must be evaluated (anterior to posterior) by sweeping the transducer over 2–2.5 cm to ensure complete evaluation. The second point is that many supraspinatus tears occur anterior near the rotator interval. This is why the modified Crass view is effective. When imaging the supraspinatus tendon, it is ideal to begin just anterior to the supraspinatus over the rotator interval and the long head of the biceps brachii tendon. This ensures that the most anterior aspect of the supraspinatus has been included so as to not overlook a tear. In addition, once the long axis of the biceps tendon is in plane (Fig 8c), this establishes the long-axis plane of the supraspinatus so that the transducer is then simply moved posterior over the tuberosity in the same imaging plane to complete evaluation of the supraspinatus tendon. Several

Figure 7

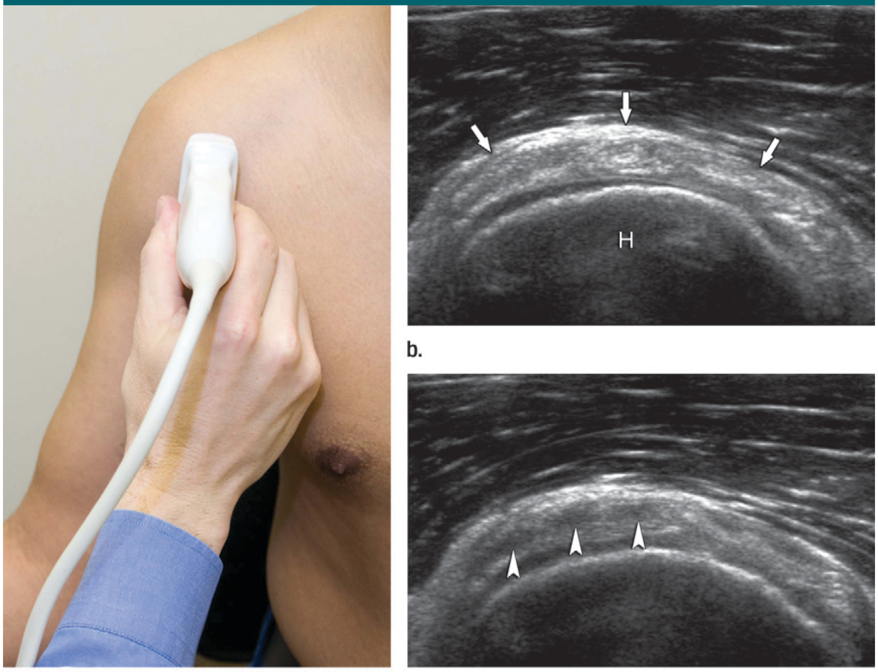

a. b. c.

Figure 7: Subscapularis tendon (short axis). **(a)** Transducer placement with shoulder externally rotated. **(b)** Corresponding US image shows hyperechoic and fibrillar subscapularis tendon (arrows). *H* = humeral head. Right side of image is inferior. **(c)** US image shows hypoechoic tendon bundles from anisotropy (arrowheads) when not imaged perpendicular to the sound beam.

Figure 8

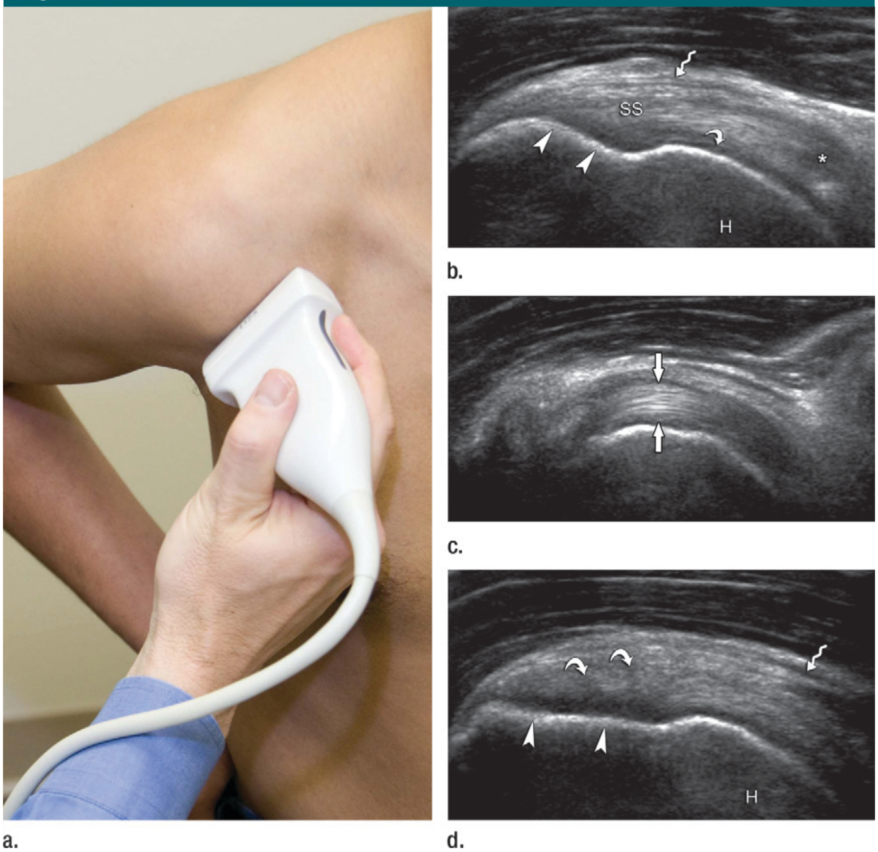

Figure 8: Supraspinatus tendon (long axis). **(a)** Transducer placement with shoulder in modified Crass position. **(b)** Corresponding US image over superior facet of greater tuberosity shows hyperechoic and fibrillar supraspinatus tendon *(SS)*, demonstrating hypoechoic anisotropy where the tendon is oblique (*). Note superior facet (arrowheads), hyaline articular cartilage (curved arrow), and collapsed hypoechoic subacromial-subdeltoid bursa (squiggly arrow). *H* = humeral head. Right side of image is medial. **(c)** US image over rotator interval shows long head of biceps brachii tendon (arrows). **(d)** US image over middle facet of greater tuberosity shows flattening of the greater tuberosity (arrowheads) relative to the humeral head *(H)*. Squiggly arrow = subacromial-subdeltoid bursa. Note hypoechoic lines (curved arrows) from anisotropy at the junction of the supraspinatus and infraspinatus.

images are obtained sequentially from anterior to posterior over the greater tuberosity, focusing not only distally at the footprint but also more proximally as well. The position of the transducer over the superior and middle facets of the greater tuberosity becomes apparent on the US images; the angle between the curved articular surface of the humeral head and the tuberosity surface has a more defined angle at the superior facet (Fig 8b) compared with the middle facet (Fig 8d), where the angle is nearly flat. As the transducer is moved posterior over the middle facet of the greater tuberosity, alternating thin hypoechoic lines are seen that represent anisotropy of the infraspinatus tendon fibers, which appear as stripes on a zebra (Fig 8d). These findings allow one to identify when the transducer is moving from the supraspinatus to infraspinatus tendons. The normal supraspinatus should be fibrillar and hyperechoic with a convex superior surface. Because the tendon fibers are curving away from the sound beam, one should continually angle the US transducer and sound beam to eliminate anisotropy.

Once the supraspinatus tendon is completely evaluated in long axis, the transducer is turned 90° to obtain a short-axis view (Fig 9a). Beginning with the transducer over the articular surface of the humeral head, the smooth, round echogenic surface of the humeral head and thin layer of hypoechoic hyaline cartilage with a uniform thickness of the overlying rotator cuff are seen, which indicates that the transducer is orientated correctly in the short axis of the supraspinatus (which should also be 90° to the previous long axis plane) (Fig 9b). As discussed above, it is critical that the rotator interval is identified at the medial aspect of the cuff to ensure that the most anterior aspect of the supraspinatus is identified. In the rotator interval, the long head of the biceps brachii will be seen in short axis between the supraspinatus and subscapularis tendons. The thin hyperechoic coracohumeral ligament can be identified superficial to the long head of the biceps tendon, which contributes to the biceps pulley along with the thin and hyperechoic superior glenohumeral ligament medial to the biceps tendon. Once the intraarticular portion of the supraspinatus is evaluated, the transducer is then moved distally toward the greater tuberosity. As the articular surface terminates and the footprint of the supraspinatus is seen at the greater tuberosity, the superior and middle facets will be visualized (Fig 9c). Identification of the facets helps to accurately localize disease in the supraspinatus (over the superior facet and a portion of the middle facet) or infraspinatus (over the middle facet) tendon. As the transducer moves further distally, the supraspinatus and infraspinatus tendons will taper over the facets and then terminate.

Step 4: Acromioclavicular joint, subacromial-subdeltoid bursa, and dynamic evaluation for subacromial impingement.—To locate the acromioclavicular joint, one may simply palpate the clavicle and move laterally toward the acromion, with the transducer in the coronal plane on the body (Fig 10a). Alternatively, with the patient's hand palm up on his or her lap, the transducer can be placed in the transverse plane over the anterior shoulder to identify the bicipital groove. The transducer then can be moved superiorly, and the characteristic bone contours of the acromioclavicular joint can be seen proximal and superior to the humeral head and rotator cuff (Fig 10b). The acromioclavicular joint is evaluated for bone irregularity, narrowing, widening, or offset. If the acromioclavicular joint is widened or if there is clinical suspicion for acromioclavicular joint disruption, dynamic evaluation should be used to assess for changes in alignment. While assessing the acromioclavicular joint in long axis relative to the clavicle, the patient is asked to move his or her ipsilateral hand to the opposite shoulder. With this maneuver, the acromioclavicular joint may abnormally widen or offset or may cause a bone-on-bone contact between the acromion and clavicle, which can be associated with symptoms.

Dynamic evaluation is then used to assess for subacromial impingement. The transducer is moved laterally from the acromioclavicular joint and is positioned over the lateral edge of the acromion (Fig 11a). With the bone landmarks of the greater tuberosity and the lateral acromion in view (Fig 11b), the patient is asked to actively elevate the arm to his or her side (Fig 11c). In may be helpful to first perform this dynamic evaluation with passive arm elevation to control patient movement. During active arm elevation, the supraspinatus tendon and overlying subacromial-subdeltoid bursa should slide smoothly under the acromion (Fig 11d) and out of view. Pooling of bursal fluid at the lateral acromion edge or snapping of bursal tissue indicates subacromial impingement (19). Other findings of impingement include interposition of the supraspinatus tendon between the greater tuberosity and the acromion, as well as direct contact between the greater tuberosity and the acromion. Dynamic evaluation for subacromial impingement can also be completed with the patients raising their arm anterolateral in front of their body, with their hand in pronation.

Step 5: Infraspinatus, teres minor, and posterior labrum.—To evaluate the infraspinatus tendon, the hand is returned to the patient's lap, palm up. In this neutral position, the transducer is placed just below the scapular spine over the posterior shoulder in a slightly oblique axial plane that parallels the orientation of the scapular spine (Fig 12a). This position will produce a long-axis view of the infraspinatus tendon, which is assessed at its insertion on the

Figure 9

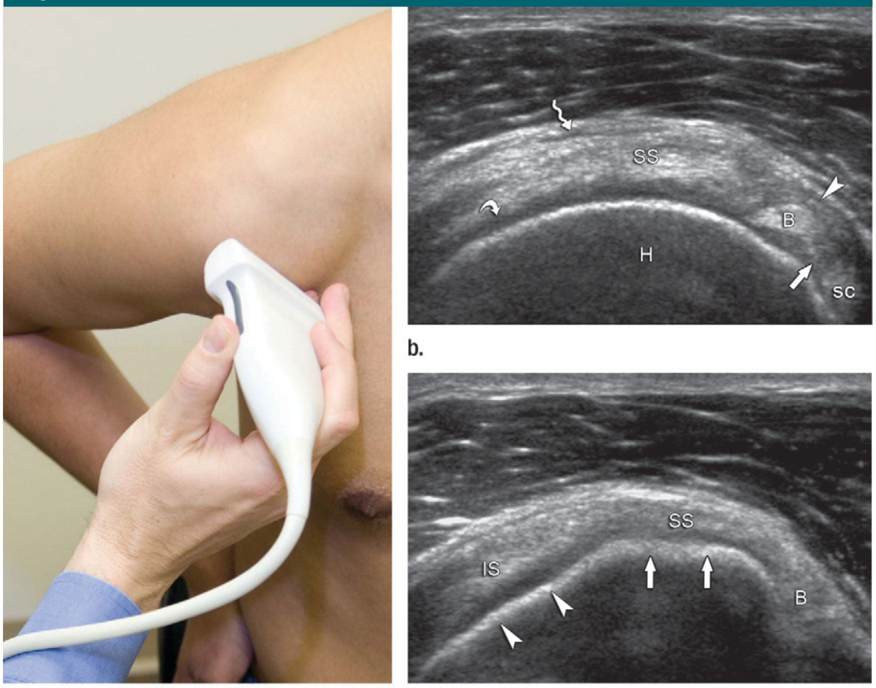

a. b. c.

Figure 9: Supraspinatus tendon (short axis). **(a)** Transducer placement with shoulder in modified Crass position. **(b)** Corresponding US image over humeral head shows hyperechoic and fibrillar supraspinatus tendon *(SS)*. Note biceps brachii tendon *(B)* in the rotator interval with superficial coracohumeral ligament (arrowhead) and medial superior glenohumeral ligament (arrow). *SC* = subscapularis tendon, curved arrow = hyaline articular cartilage, squiggly arrow = subacromial-subdeltoid bursa, *H* = humeral head. Right side of image is anterior. **(c)** US image distal to articular surface over greater tuberosity facets shows supraspinatus tendon *(SS)* adjacent to superior facet (arrows), and infraspinatus tendon *(IS)* adjacent to middle facet of greater tuberosity (arrowheads). Note biceps brachii tendon *(B)*. Right side of image is anterior.

Figure 10

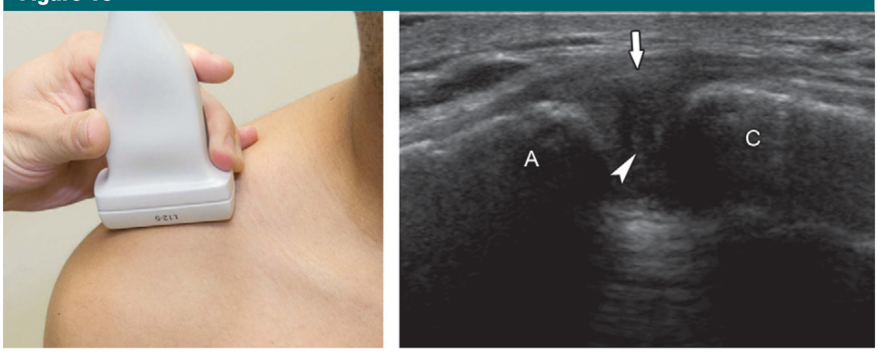

a. b.

Figure 10: Acromioclavicular joint. **(a)** Transducer placement over superior aspect of the shoulder. **(b)** Corresponding US image shows acromioclavicular joint (arrow) with characteristic hyperechoic bone contours of the distal clavicle *(C)* and acromion *(A)*. Note echogenic fibrocartilage disc (arrowhead). Left side of image is lateral.

Figure 11

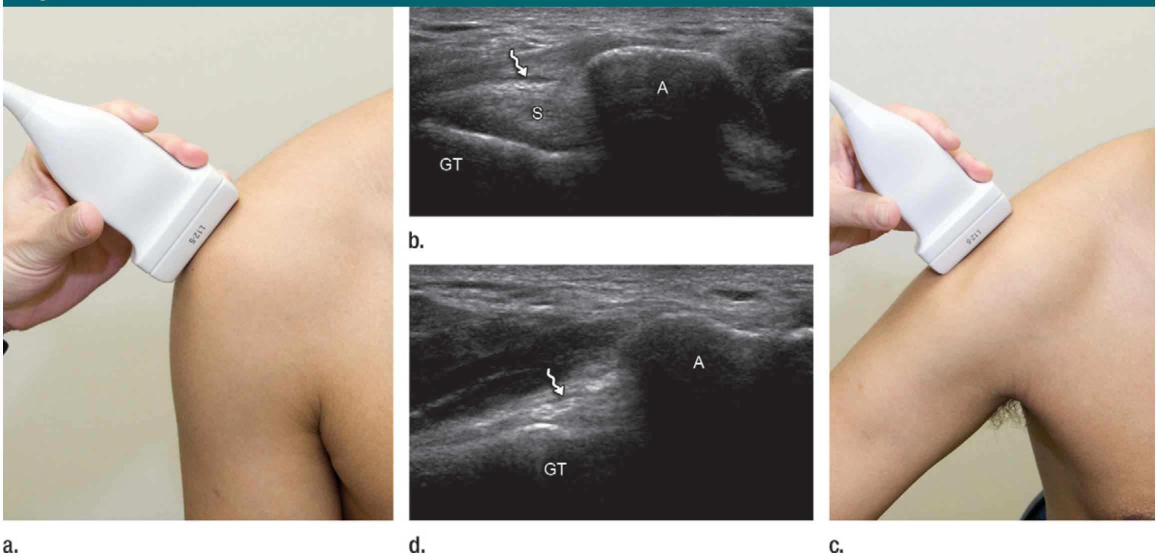

Figure 11: Dynamic assessment for subacromial impingement. **(a)** Transducer placement over superolateral aspect of shoulder in neutral position. **(b)** Corresponding US image shows acromion *(A)* and greater tuberosity *(GT)* with supraspinatus tendon *(S)* and collapsed subacromial-subdeltoid bursa (arrow). **(c)** Transducer placement after abduction of the shoulder. **(d)** US image shows acromion *(A)*, greater tuberosity *(GT)*, and normal collapsed subacromial-subdeltoid bursa (arrow). Left side of images is lateral.

Figure 12

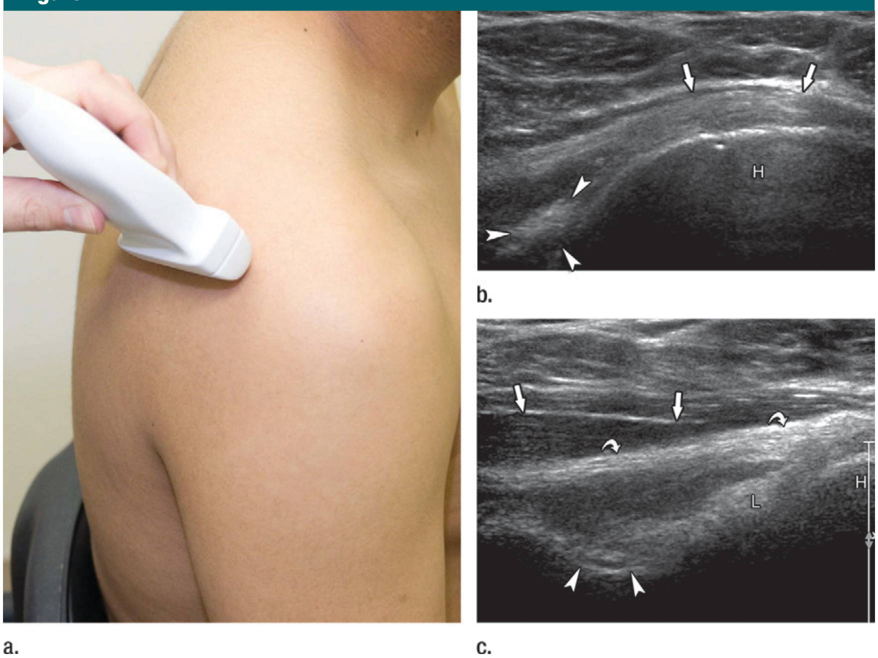

Figure 12: Infraspinatus tendon (long axis), posterior glenohumeral joint, and spinoglenoid notch. **(a)** Transducer placement over posterior aspect of the shoulder in neutral position. **(b)** Corresponding US image shows characteristic contours of the humeral head *(H)* with adjacent infraspinatus tendon (arrows) and glenoid labrum (arrowheads). **(c)** US image medial to **b** shows spinoglenoid notch (arrowheads) of scapula with adjacent suprascapular vessels. Note infraspinatus musculotendinous junction (straight arrows) and central tendon (curved arrows). *H* = humeral head, *L* = labrum. Left side of image is medial.

posterior aspect of the greater tuberosity (Fig 12b). Moving the transducer medial toward the scapula, other structures to be evaluated include the posterior labrum (for labral tear), the spinoglenoid notch (for paralabral cyst), and the posterior glenohumeral joint recess (for joint fluid or synovitis) (Fig 12c). The transducer is then rotated 90° (Fig 13a) to assess the infraspinatus tendon in short axis (Fig 13b). If visualization of the distal infraspinatus tendon is difficult due to shadowing from the acromion, it is often helpful to have the patient place his or her ipsilateral hand on the contralateral shoulder. The advantage of this maneuver is that the distal infraspinatus tendon will be pulled anterior to allow visualization. The disadvantage of this internal rotation position is that the infraspinatus tendon, which was linear in the neutral position, is now curved as it wraps around the posterior humerus to the relatively anteriorly located greater tuberosity. If one continues to have difficulty in identifying the infraspinatus tendon, an additional scanning method can be used, which begins by palpating the spine of the scapula over the posterior shoulder. The transducer is then placed in the

Figure 13

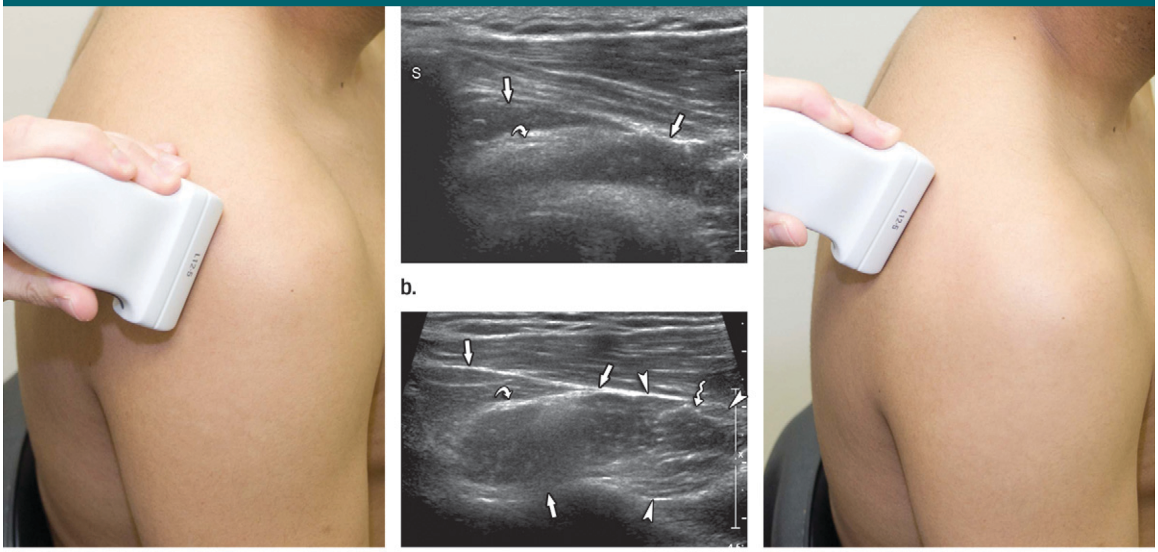

a. d. c.

Figure 13: Infraspinatus and teres minor (short axis). **(a)** Transducer placement over posterior aspect of the shoulder in neutral position. **(b)** Corresponding US image shows infraspinatus (straight arrows) and central tendon (curved arrow). *S* = scapular spine. Left side of image is superior. **(c)** Transducer placement medial to **a. (d)** Corresponding US image shows infraspinatus (straight arrows) with central tendon (curved arrow) and teres minor (arrowheads) with more superficial tendon (squiggly arrow). Left side of image is cephalad.

sagittal plane just inferior to the scapular spine, and the large muscle belly of the infraspinatus is seen. Once the echogenic central tendon is identified in short axis, the transducer is turned 90° to align the tendon in long axis, and the transducer is moved lateral to the greater tuberosity. External rotation of the shoulder while imaging the posterior shoulder recess is helpful to visualize small amounts of glenohumeral joint fluid.

In addition to evaluating the infraspinatus tendon for tear, it is important to evaluate for fatty degeneration and atrophy of the infraspinatus muscle in the setting of a rotator cuff tear as this finding indicates higher likelihood of failure after rotator cuff repair (20). The transducer is moved medially over the musculotendinous junction of the infraspinatus in short axis (Fig 13c). The diagnosis of fatty degeneration or atrophy is made by comparing the size and echogenicity of the infraspinatus muscle at the muscle-tendon junction with the adjacent teres minor muscle. Normally, the infraspinatus muscle size should be approximately twice that of the teres minor at the musculotendinous junction and the hypoechoic muscle echogenicity should be similar (Fig 13d). Relative increased echogenicity of the infraspinatus muscle indicates fatty degeneration and decreased size indicates atrophy. By moving the transducer superiorly over the scapular spine, the adjacent supraspinatus muscle should also be assessed for fatty degeneration and atrophy (21). Of note, relative increased echogenicity and decreased size of the teres minor muscle can be seen with quadrilateral space syndrome or may be idiopathic. Once the teres minor is identified, this structure can also be evaluated at its greater tuberosity insertion.

Pitfalls

There are several scanning pitfalls that, although have been introduced above, deserve further emphasis. The most common and most problematic pitfall relates to anisotropy, where the normal hyperechoic tendon appears artifactually hypoechoic when the tendon is not perpendicular to the sound beam. As little as 2°–3° of angulation will produce this artifact, as the ultrasound beam is reflected away from the transducer (22). This artifact is especially problematic when evaluating the supraspinatus tendon, as it is curved to its insertion following the contours of the adjacent humeral head (Fig 8b). Anisotropy is also seen when imaging the long head of the biceps brachii tendon in the bicipital groove (Figs 4c, 5c).

Another pitfall is incomplete evaluation of the rotator cuff. One must remember that the greater tuberosity is several centimeters in width (anterior to posterior), and this entire distance must be evaluated both in long and short axis relative to the supraspinatus tendon (Fig 9c). Additionally, visualization of the long head of the biceps tendon in the rotator interval is critical to ensure that the most anterior aspect of the supraspinatus tendon is evaluated, as many tears involve this area (Fig 9b).

One additional pitfall relates to misinterpretation of normal tendons. At the posterior aspect of the rotator cuff, it is common to see alternating hypoechoic bands at the junction of the supraspinatus and infraspinatus tendons from anisotropy. In addition, hypoechoic bands are seen when evaluating the subscapularis tendon in short axis related to anisotropy of its multiple tendons (Fig 7c).

Each of these findings should not be misinterpreted as tendon disease.

In conclusion, keys to a successful shoulder US examination include understanding the anatomy, imaging the structures of interest in long and short axis, eliminating artifacts, and then evaluating for disease, following a standardized imaging protocol. This will ensure a thorough, comprehensive, and efficient evaluation of the rotator cuff.

Disclosures of Potential Conflicts of Interest: **J.A.J.** Financial activities related to the present article: none to disclose. Financial activities not related to the present article: paid consultant to BioClinica, received payment for lectures including service on speakers bureaus and for manuscript preparation; institution has grants/grants pending from American Institute of Ultrasound in Medicine. Other relationships: received royalties from Elsevier Publishers.

References

1. Martinoli C, Bianchi S, Prato N, et al. US of the shoulder: non-rotator cuff disorders. RadioGraphics 2003;23(2):381–401; quiz 534.
2. Moosikasuwan JB, Miller TT, Burke BJ. Rotator cuff tears: clinical, radiographic, and US findings. RadioGraphics 2005;25(6):1591–1607.
3. Teefey SA, Hasan SA, Middleton WD, Patel M, Wright RW, Yamaguchi K. Ultrasonography of the rotator cuff: a comparison of ultrasonographic and arthroscopic findings in one hundred consecutive cases. J Bone Joint Surg Am 2000;82(4):498–504.
4. Vlychou M, Dailiana Z, Fotiadou A, Papanagiotou M, Fezoulidis IV, Malizos K. Symptomatic partial rotator cuff tears: diagnostic performance of ultrasound and magnetic resonance imaging with surgical correlation. Acta Radiol 2009;50(1):101–105.
5. Le Corroller T, Cohen M, Aswad R, Pauly V, Champsaur P. Sonography of the painful shoulder: role of the operator's experience. Skeletal Radiol 2008;37(11):979–986.
6. Jamadar DA, Jacobson JA, Caoili EM, et al. Musculoskeletal sonography technique: focused versus comprehensive evaluation. AJR Am J Roentgenol 2008;190(1):5–9.
7. VandenBerghe G, Hoenecke HR, Fronek J. Glenohumeral joint instability: the orthopedic approach. Semin Musculoskelet Radiol 2005;9(1):34–43.
8. Minagawa H, Itoi E, Konno N, et al. Humeral attachment of the supraspinatus and infraspinatus tendons: an anatomic study. Arthroscopy 1998;14(3):302–306.
9. Mochizuki T, Sugaya H, Uomizu M, et al. Humeral insertion of the supraspinatus and infraspinatus: new anatomical findings regarding the footprint of the rotator cuff. Surgical technique. J Bone Joint Surg Am 2009;91(Suppl 2 Pt 1):1–7.
10. Erickson SJ. High-resolution imaging of the musculoskeletal system. Radiology 1997;205(3):593–618.
11. Ruotolo C, Fow JE, Nottage WM. The supraspinatus footprint: an anatomic study of the supraspinatus insertion. Arthroscopy 2004;20(3):246–249.
12. Dugas JR, Campbell DA, Warren RF, Robie BH, Millett PJ. Anatomy and dimensions of rotator cuff insertions. J Shoulder Elbow Surg 2002;11(5):498–503.
13. Jin W, Ryu KN, Park YK, Lee WK, Ko SH, Yang DM. Cystic lesions in the posterosuperior portion of the humeral head on MR arthrography: correlations with gross and histologic findings in cadavers. AJR Am J Roentgenol 2005;184(4):1211–1215.
14. Morag Y, Jacobson JA, Shields G, et al. MR arthrography of rotator interval, long head of the biceps brachii, and biceps pulley of the shoulder. Radiology 2005;235(1):21–30.
15. Simovitch R, Sanders B, Ozbaydar M, Lavery K, Warner JJ. Acromioclavicular joint injuries: diagnosis and management. J Am Acad Orthop Surg 2009;17(4):207–219.
16. Magnavita N, Bevilacqua L, Mirk P, Fileni A, Castellino N. Work-related musculoskeletal complaints in sonologists. J Occup Environ Med 1999;41(11):981–988.
17. Crass JR, Craig EV, Feinberg SB. The hyperextended internal rotation view in rotator cuff ultrasonography. J Clin Ultrasound 1987;15(6):416–420.
18. Ferri M, Finlay K, Popowich T, Stamp G, Schuringa P, Friedman L. Sonography of full-thickness supraspinatus tears: comparison of patient positioning technique with surgical correlation. AJR Am J Roentgenol 2005;184(1):180–184.
19. Bureau NJ, Beauchamp M, Cardinal E, Brassard P. Dynamic sonography evaluation of shoulder impingement syndrome. AJR Am J Roentgenol 2006;187(1):216–220.
20. Morag Y, Jacobson JA, Miller B, De Maeseneer M, Girish G, Jamadar D. MR imaging of rotator cuff injury: what the clinician needs to know. RadioGraphics 2006;26(4):1045–1065.
21. Khoury V, Cardinal E, Brassard P. Atrophy and fatty infiltration of the supraspinatus muscle: sonography versus MRI. AJR Am J Roentgenol 2008;190(4):1105–1111.
22. Crass JR, van de Vegte GL, Harkavy LA. Tendon echogenicity: ex vivo study. Radiology 1988;167(2):499–501.